BMC Chemistry

RESEARCH

Open Access

Silica/APTPOSS anchored on $MnFe_2O_4$ as an efficient nanomagnetic composite for the preparation of spiro-pyrano [2, 3-c] chromene derivatives

Samira Moein-Najafabadi[1] and Javad Safaei-Ghomi[1*]

Abstract

The synthesis of Octakis [3- (3-amino propyl triethoxysilane) propyl] octa-silsesquioxane (APTPOSS), a derivative of polyhedral oligomeric silsesquioxane, was utilized to produce an efficient nanocomposite. MNPs@Silica/APTPOSS was characterized through scanning electron microscopy, Fourier transform infrared spectroscopy, vibrating sample magnetometry, X-ray diffraction, and Thermogravimetric analysis. These magnetic nanoparticles, a combination of organic-inorganic hybrid polyhedral oligomeric silsesquioxane, were utilized as a proficient heterogeneous catalyst in the one-pot synthesis of spirooxindoles derivatives. Furthermore, they could be swiftly isolated and reused six times while maintaining their catalytic efficiency.

Keywords Nanocomposite, Oligomeric silsesquioxane, Heterogeneous, One-pot synthesis, Spirooxindoles

Introduction

Utilizing heterogeneous catalysts has emerged as a valuable approach for addressing multiple challenges, such as catalyst retrieval, product isolation, environmental impact, and elevated reaction temperatures [1, 2]. In this context, the utilization of nanometals as catalysts has experienced rapid expansion, leading to the development of numerous active and efficient nanocatalysts with distinct advantages over traditional catalysts, including enhanced activity and durability [3–5].

Magnetic nanoparticles (MNPs) are promising support materials for heterogeneous catalysts because of their straightforward synthesis, large surface area, great thermal and chemical stability, potential for surface modification, low toxicity, and cost-effectiveness [6–10]. Additionally, employing an external magnet allows for easy separation of catalyst-loaded MNPs from reaction products, eliminating filtration and simplifying catalyst recycling [11].

Octakis [3-(3aminopropyltriethoxysilane) propyl] octa-silsesquioxane, commonly abbreviated as APTPOSS, is a silsesquioxane-based organic-inorganic hybrid material [12]. It consists of a central silicon atom surrounded by eight organic groups, each containing an amino group and three ethoxy groups. APTPOSS is a versatile material with a wide range of potential applications due to its unique properties. APTPOSS is often employed as a surface modifier or coating agent due to its ability to form strong bonds with organic and inorganic substrates [13]. The organic groups on its surface provide functional groups that can easily react with other molecules, allowing for tailored surface modifications. This property

*Correspondence:
Javad Safaei-Ghomi
safaei@kashanu.ac.ir
[1]Department of Organic Chemistry, Faculty of Chemistry, University of Kashan, P.O. Box 87317-51167, Kashan, I. R. of Iran

makes APTPOSS useful in adhesion promotion, surface functionalization, and the development of hybrid materials [14, 15].

In addition to its surface modification capabilities, APTPOSS also exhibits excellent thermal stability and mechanical strength. The inorganic silica core provides a rigid framework that enhances the material's durability and resistance to high temperatures. This makes APTPOSS suitable for applications in harsh environments or where high-temperature stability is required [16].

Furthermore, APTPOSS possesses interesting optical properties, including high transparency in the visible and near-infrared regions of the electromagnetic spectrum. This characteristic makes it a promising material for optical applications such as lenses, coatings, and optoelectronic devices [17]. Overall, Octakis [3-(3 aminopropyl triethoxysilane) propyl] octasilsesquioxane (APTPOSS) is a versatile hybrid material with a wide range of potential applications. Its unique combination of organic and inorganic components, excellent surface modification capabilities, thermal stability, mechanical strength, and optical properties, make it a valuable material for various industries and research fields [18, 19].

The indole scaffold is a bicyclic heterocyclic organic compound. It is a structural component of the amino acid tryptophan found in many natural products and pharmaceuticals [20, 21]. Indoles exhibit diverse biological activities, including anti-inflammatory, anti-cancer, and anti-depressant properties [22]. The indole scaffold is also found in many synthetic compounds, such as the dye indigo and the drug LSD [23]. Indoles are an important class of compounds with a wide range of applications in the pharmaceutical, agricultural, and materials science industries (Fig. 1) [24–26].

Utilizing the one-pot multicomponent reaction protocol is a highly effective approach for achieving optimal synthesis due to its advantages in time and energy efficiency, high atom efficiency, and ease of execution [27]. Nitrogen-containing heterocyclic compounds are important in organic synthesis and medicinal chemistry [28, 29]. Among these, spirooxindole derivatives are valuable fused heterocycles that are essential building blocks for synthetic compounds, natural products, and pharmaceutical molecules [30, 31]. While various practical methods have been explored to prepare spiro 4 H-pyrans, each method comes with its own set of advantages and limitations that restrict their applicability [32, 33]. Therefore, developing a new efficient strategy for producing these fused heterocyclic structures is imperative. Building upon our previous research endeavors [34–36], we present a straightforward approach for fabricating $MnFe_2O_4$@SiO_2/APTPOSS as a powerful catalyst for the one-pot reaction involving activated methylene compounds, 1,3 dicarbonyl compounds, and isatins under mild conditions (Fig. 2).

Results and discussion

Structural analysis of the $MnFe_2O_4$@SiO_2/APTPOSS as the catalyst

Figure 3 demonstrates the sequential process for immobilizing $MnFe_2O_4$ with a Polyhedral Oligomeric Silsesquioxanes-based inorganic-organic hybrid. The MNPs ($MnFe_2O_4$) were first synthesized using a co-precipitation method in a basic solution. It is known that the surface of the MNPs can be functionalized using various surface modifiers. Subsequently, octakis (3 chloropropyl) octasilsesquioxane was synthesized through hydrolyzing 3-chloropropyltrimethoxysilane in an acidic environment. React ClPOSS with 3-aminopropyltriethoxysilane to produce APTPOSS. The final step involved treating $MnFe_2O_4$ with an aminopropyltriethoxysilane derivative and TEOS. The $MnFe_2O_4$@SiO_2/APTPOSS was distinguished using TEM, SEM, VSM, Fourier transform infrared (FT-IR) analysis, TGA, and X-ray diffraction (XRD) techniques.

Figure 4 illustrates the X-ray diffraction patterns of the synthesized APTPOSS, $MnFe_2O_4$, and $MnFe_2O_4$@SiO_2/APTPOSS. The XRD patterns of the $MnFe_2O_4$ nanoparticles with and without POSS show consistent peaks, indicating that the crystalline spinel structure of $MnFe_2O_4$ is preserved during the APTPOSS coating process. Specifically, the X-ray diffraction (XRD) patterns reveal six

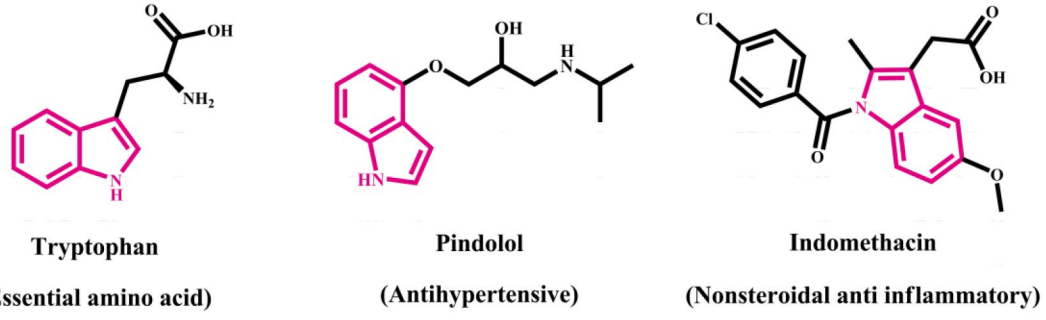

Fig. 1 Indole scaffold in physiologically and pharmacologically relevant substances

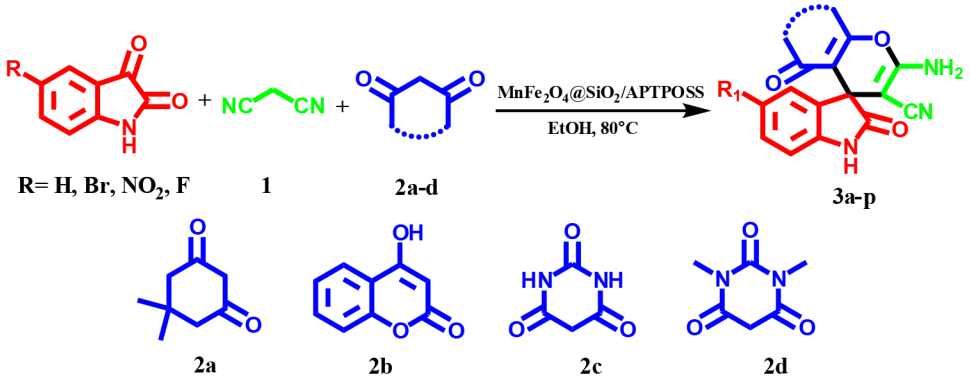

Fig. 2 Synthesis of spirooxindole using MNPs@SiO_2/APTPOSS

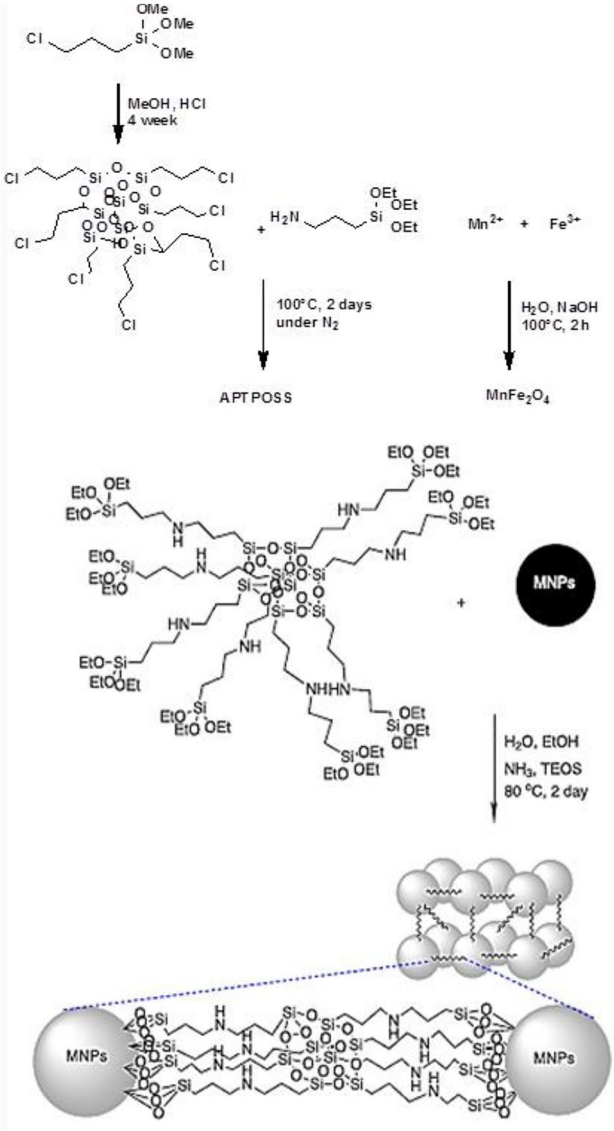

Fig. 3 Preparation routes to $MnFe_2O_4$@SiO_2/APTPOSS nanoparticles

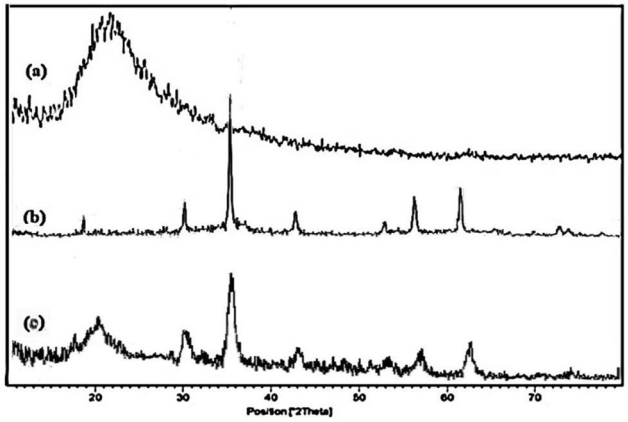

Fig. 4 The X-ray diffraction patterns of (**a**) APTPOSS, (**b**) $MnFe_2O_4$ and (**c**) $MnFe_2O_4$@SiO_2/APTPOSS

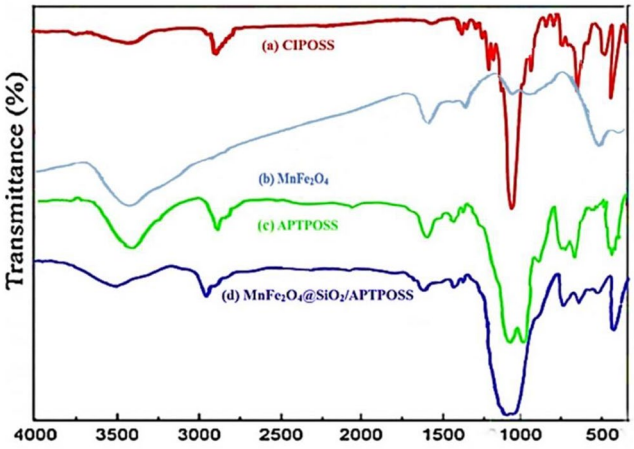

Fig. 5 Fourier transform-infrared (FT-IR) spectra of (**a**) ClPOSS, (**b**) $MnFe_2O_4$, (**c**) APTPOSS and (**d**) $MnFe_2O_4$@SiO_2/APTPOSS

characteristic peaks corresponding to a cubic phase of manganese iron oxide at 2θ values of 30.18°, 35.97°, 43.22°, 53.92°, 57.42°, and 63.03° for both $MnFe_2O_4$ and $MnFe_2O_4$@SiO_2/APTPOSS in Fig. 4(b) and (c). Additionally, the broad peaks observed in Fig. 4(a) and (c) at 2θ values ranging from 16° to 28° are attributed to an amorphous Si-O bond.

The Fourier transform infrared spectra in Fig. 5 illustrate the characteristic features of ClPOSS, $MnFe_2O_4$, APTPOSS, and $MnFe_2O_4$@SiO_2/APTPOSS. Notable features of the ClPOSS molecules include peaks at 2955 cm^{-1} (C-H bond stretching), 1102 cm^{-1} (Si-O-Si band stretching), and 810 cm^{-1} (C-Cl bond stretching). Figure 5(b) and (d) show common features, including peaks at 489, 576, 3437, and 1627 cm^{-1}, which depict the stretching vibrations of Mn-O bonds, Fe-O bonds, O-H bonds, and O-H bond bending. The successful incorporation of Silica/ POSS-based inorganic-organic hybrid on the surface of $MnFe_2O_4$ is indicated by broad peaks around 1000–1160 cm^{-1} associated with Si-O bond stretching vibrations. Additionally, C-H bond stretching at 2915–2965 cm^{-1} and C-H bond bending vibration at approximately 1470 cm^{-1} is observed in Fig. 5(c) and (d).

Figure 6 illustrates the TGA analysis of $MnFe_2O_4$@SiO_2/APTPOSS. It demonstrates a decline in weight of approximately 28% between 200 and 500 °C, which can associated with the degradation of the organic components. Consequently, the catalyst exhibits stability up to less than 200 °C, affirming its suitability for application in organic reactions at temperatures around 80 °C.

The FE-SEM images in Fig. 7 compare the magnetic nanoparticles. As depicted in Fig. 7(a), the uncoated $MnFe_2O_4$ seeds have a size of about 38 nm and display acceptable uniformity. The SEM image in Fig. 7(b) indicates the $MnFe_2O_4$ coated with SiO_2/POSS have preserved their morphology, but this does not apply to particle size and aggregation. The observed accumulation and alterations in particle size lead to the conclusion that the nanocatalyst has been effectively synthesized.

To investigate more accurately the morphology of $MnFe_2O_4$@SiO_2/APTPOSS nanocomposites, TEM analysis was applied (Fig. 8). TEM images confirmed that the

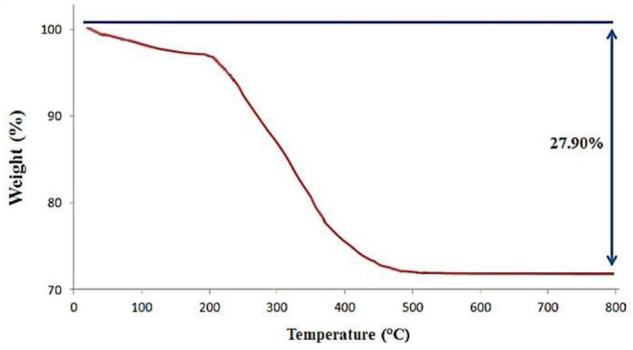

Fig. 6 Thermal gravimetric analysis of $MnFe_2O_4$@SiO_2/APTPOSS

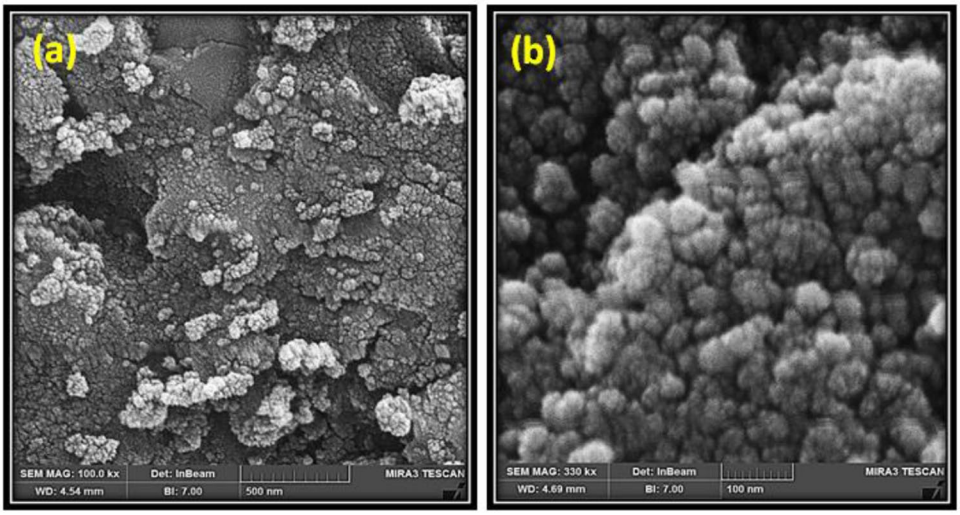

Fig. 7 The FE-SEM images of (**a**) $MnFe_2O_4$ and (**b**) $MnFe_2O_4$@SiO_2/APTPOSS

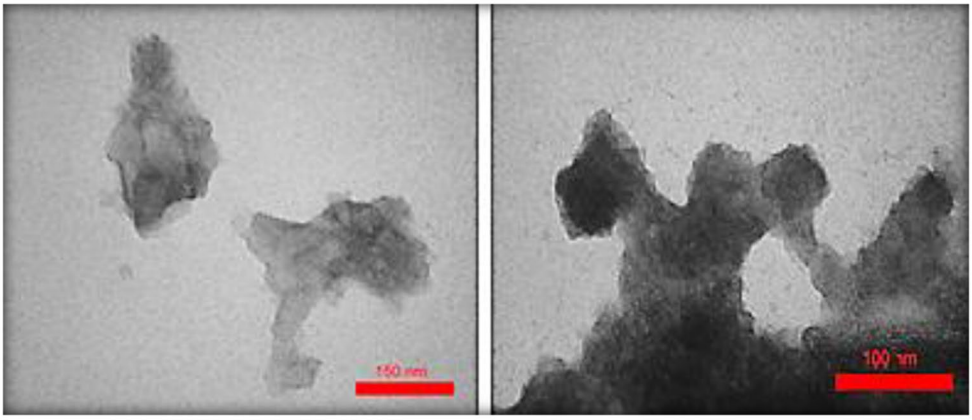

Fig. 8 The TEM images of $MnFe_2O_4$@SiO_2/APTPOSS

magnetic nanocomposites have spherical morphology with uniform distribution.

The magnetic characteristics of $MnFe_2O_4$ and MNPs@SiO_2/APTPOSS were examined using a vibrating sample magnetometer at room temperature (Fig. 9). The magnetization hysteresis loops for two samples are S-like and show superparamagnetic properties for them. The saturation magnetization (Ms) is 32.5 Oe for $MnFe_2O_4$ and 21.8 Oe for MNPs@SiO_2/APTPOSS. The magnetic saturation value decreases by approximately 10.7 mug^{-1} following the coating process, possibly attributed to the

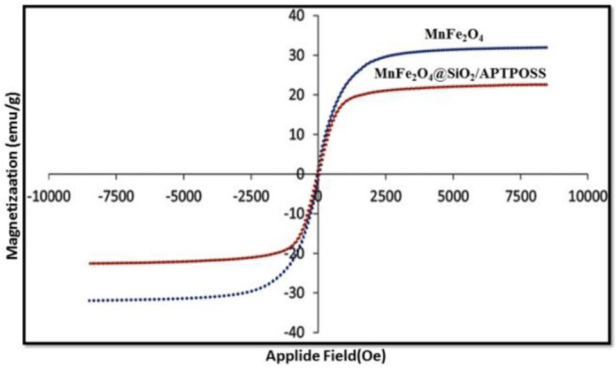

Fig. 9 Comparison of VSM analysis for $MnFe_2O_4$ and MNPs@SiO_2/APTPOSS

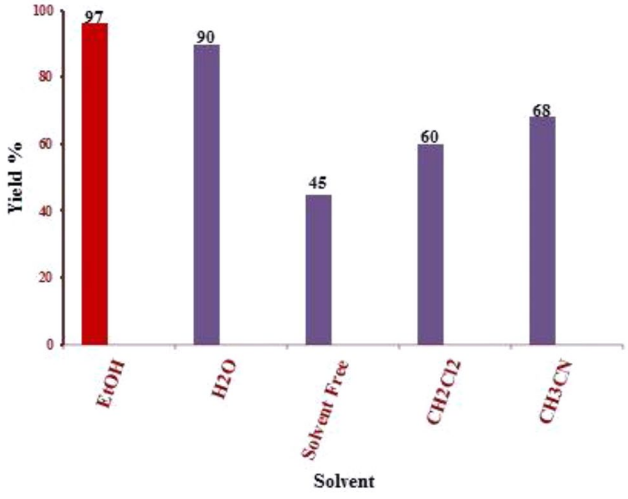

Fig. 10 The impact of various solvents on the preparation of oxindole using $MnFe_2O_4$@SiO_2/APTPOSS

enhanced surface area facilitating successful nanoparticle coating with SiO_2 and APTPOSS.

Different solvents were used to examine the reactivity of isatin derivatives, 1, 3-dicarbonyl compounds (2a-d), and malononitrile 1. A good yield was achieved when the reaction was conducted in ethanol (Fig. 10). Subsequently, the reaction was carried out using different catalysts and without a catalyst. It was found that $MnFe_2O_4$@SiO_2/APTPOSS was the most effective catalyst, resulting in a 96% yield of product 3a. The impact of catalyst loading was then investigated using 5 mg and 15 mg of $MnFe_2O_4$@SiO_2/APTPOSS, respectively. The experimental findings indicated that using 10 mg of $MnFe_2O_4$@SiO_2/APTPOSS as a catalyst yielded the most favorable results. Any deviation from this particular catalyst loading, whether reduced or increased, resulted in a drop in the total product yield.

Various reaction conditions were explored in the experimental model involving isatin, dimedone, and malononitrile to achieve optimal production yield and showcase the effectiveness of the catalyst. The results indicated that conducting the reaction at 80°C with 10 mg of the catalyst ($MnFe_2O_4$@SiO_2/APTPOSS) in ethanol as the solvent leads to an enhanced production yield (Table 1, entry 5).

Table 2 displays the results obtained from the synthesis of various spiro[indoline-3,4'-pyrano[3,2-c] chromene], spiro[indoline-3,5'-pyrano[2,3-d]pyrimidine], and spiro[chromene-4,3'-indolines] compounds. The reactions took place in ethanol as a solvent at a temperature of 80°C, using isatin derivatives and different 1, 3-dicarbonyls.

The catalyst's reusability is a well-established property of significant importance. Our study focused on utilizing MNPs@SiO_2/APTPOSS as a catalyst in optimized conditions. Following the reaction, the catalyst was washed with acetone and methanol and dried in an oven at 65 °C for 70 min. It was then directly used with new substrates under the same conditions. The results demonstrate that the catalyst was effectively employed in six consecutive reaction cycles without a noticeable decrease in product yield, showing initial yields of 97% and 90% by the sixth cycle (Fig. 11).

Table 1 Reported catalytic system for the formation of spirooxindole derivatives[a]

Entry	Catalyst	Solvent/ Temp. (°C)	Time (min)	Yield[b] (%)	Ref.
1	-	EtOH / 80	90	30	This work
2	$MnFe_2O_4$@SiO_2 (20 mg)	EtOH / 80	40	60	This work
3	$MnFe_2O_4$@SiO_2/APTPOSS (10 mg)	EtOH / 50	20	75	This work
4	$MnFe_2O_4$@SiO_2/APTPOSS (10 mg)	Solvent-free / 80	15	80	This work
5	**$MnFe_2O_4$@SiO_2/APTPOSS (10 mg)**	**EtOH / 80**	**10**	**97**	**This work**
6	$MnFe_2O_4$@SiO_2/APTPOSS (10 mg)	EtOH / 90	reflux	94	This work
7	$MnFe_2O_4$@SiO_2/APTPOSS (10 mg)	H_2O / 80	30	70	This work
8	Amino-appended b-cyclodextrin (5 mol%)	H_2O / RT	7 h	91	[37]
9	THAM (30 mol%)	EtOH / RT	4 h	94	[38]
10	TiO_2-CNTs (24 mg)	H_2O / RT	6 h	94	[39]

Bold entry is the best one of the experiment

[a] Reaction conditions: isatin (1mmol), malononitrile (1 mmol), and 1,3 dicarbonyl compounds (1 mmol) in presence $MnFe_2O_4$@SiO_2/APTPOSS (10 mg) in EtOH under reflux conditions

[b] Isolated yields

A plausible mechanism for the preparation of spiro oxindole

A potential mechanism is suggested for the one-step synthesis of 2-amino-7, 7-dimethyl-2',5-dioxo-5,6,7,8 tetrahydrospiro[chromene-4,3'-indoline]-3-carbonitrile via a three-component reaction. At first, an acidic catalytic method was employed to carry out the Knoevenagel condensation and form intermediate (A) Then, intermediate A underwent a Michael addition with dimedone to produce intermediate (B) Finally, the target product (3a) was generated through intramolecular cyclization. At the end of the reaction, the catalyst could be recovered by external permanent magnet (Fig. 12).

Conclusions

We were able to effectively synthesize composite nanoparticles in our research by blending manganese iron oxide MNPs ($MnFe_2O_4$) with APTPOSS, resulting in the production of oxindoles. The reaction was efficiently carried out quickly and with minimal catalyst usage. Moreover, the resulting catalyst exhibited numerous benefits, including long-term stability, exceptional catalytic activity for this specific reaction, effortless separation of the catalyst through an external magnetic field, and straightforward work-up procedures. Additionally, the catalyst can be conveniently retrieved and reused multiple times without experiencing a noticeable decline in its catalytic effectiveness. The present method is expected to apply to generating diverse libraries because of the plentiful availability of isatins and 1, 3-dicarbonyl compounds. Overall, the widespread adoption of this technique in combinatorial chemistry and drug discovery holds great promise for advancing the development of new pharmaceutical agents and improving treatment options for various medical conditions.

Experimental section

General

All chemicals and solvents utilized in the investigation were procured commercially and were not subjected to further purification. Fourier transform infrared (FT IR) spectroscopy was analyzed using a Nicolet Magna-400 spectrometer with KBr pellets. ^{1}H NMR data were gathered in DMSO-d6 using a Bruker DRX 400 spectrometer with tetramethylsilane as the internal reference. Powder X-ray diffraction (XRD) was performed using a Philips X'pert diffractometer with monochromatized Cu Kα radiation (λ = 1.5406 Å). Additionally, the magnetic properties of magnetite nanoparticles were measured utilizing a vibrating sample magnetometer (PPMS-9 T) at 300 K at Iran's Kashan University. The nanoparticles' morphology was investigated using field emission scanning electron microscopy (FE-SEM) with model MIRA3. The microscopic morphology of the nanoparticles was observed using a Philips transmission electron microscope (TEM) operating at 100 Kv. Thermogravimetric analysis (TGA) curves were recorded with a V5.1 A DuPont 2000.

General procedure for the synthesis of $MnFe_2O_4$ nanoparticles

Following a 30-minute exposure to nitrogen gas in 200 mL of purified, deoxygenated water, 5 g of $Mn(NO_3)_2.4H_2O$ and 14 g of $Fe(NO_3)_3.6H_2O$ were dissolved in ultrapure water with vigorous mechanical stirring. Subsequently, the mixture was agitated while 2.0 M NaOH solution was incrementally added until reaching a pH of 11. The mixture was then heated to 100 °C and maintained at this temperature for 2 h. Under the influence of an external magnetic field, a black precipitate was collected and subsequently rinsed with ultrapure water three times to eliminate contaminants such as OH^-, NO_3^-, and Na^+. Following freeze-drying, pure $MnFe_2O_4$ nanoparticles were ultimately obtained.

Preparation of ClPOSS nanoparticles

The initial substance octakis (3 chloropropyl) octasilsesquioxane was synthesized following the procedure outlined by Dittmar et al. [40]. A mixture of 3 Chloropropyltrimethoxysilane (20 g), 450 ml of methanol, and 22.5 ml of concentrated hydrochloric acid was stirred for a minimum of 4 weeks at room temperature. After this period, colorless crystals (3.6 g) were obtained, which

Table 2 Preparation of spirooxindole derivatives using $MnFe_2O_4$@SiO_2/APTPOSS catalyst[a]

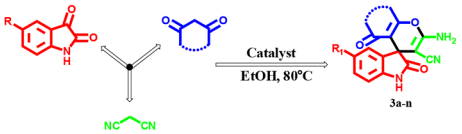

Entry	Product numbering	Substrate	Product	Time	Yield[b] (%)	M.P.(℃)
1	**3a**	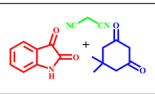	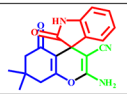	10	97	304-306
2	**3b**		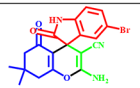	12	97	305-307
3	**3c**	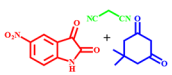	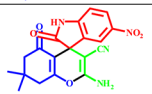	11	95	303-306
4	**3d**		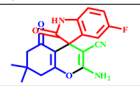	13	96	>300
5	**3e**			10	94	>300
6	**3f**	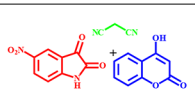	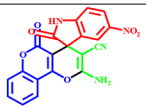	14	97	>300
7	**3g**		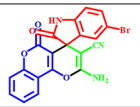	13	92	>300
8	**3h**	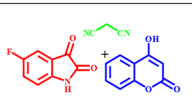	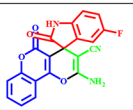	15	94	>300
9	**3i**			12	93	273-275
10	**3j**	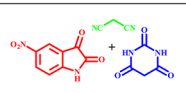	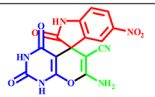	10	95	284-288
11	**3k**			14	95	209-212
12	**3l**	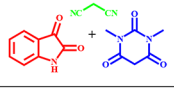	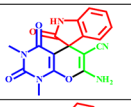	20	90	228-231
13	**3m**	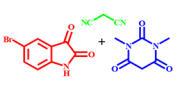	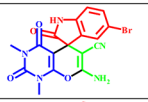	15	97	259-263
14	**3n**	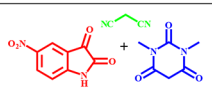	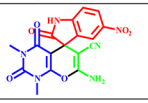	10	95	280-283

[a] Reaction conditions: isatin (1mmol), malononitrile (1 mmol), and 1,3 dicarbonyl compounds (1 mmol) in presence $MnFe_2O_4$@SiO_2/APTPOSS (10 mg) in EtOH under reflux conditions[b] Isolated yields

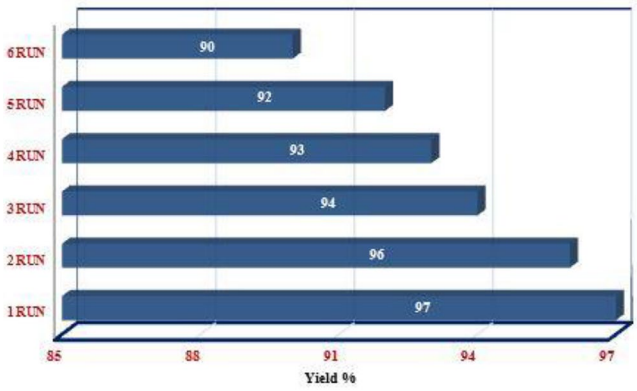

Fig. 11 Recycling of $MnFe_2O_4$@ SiO_2/APTPOSS as the catalyst

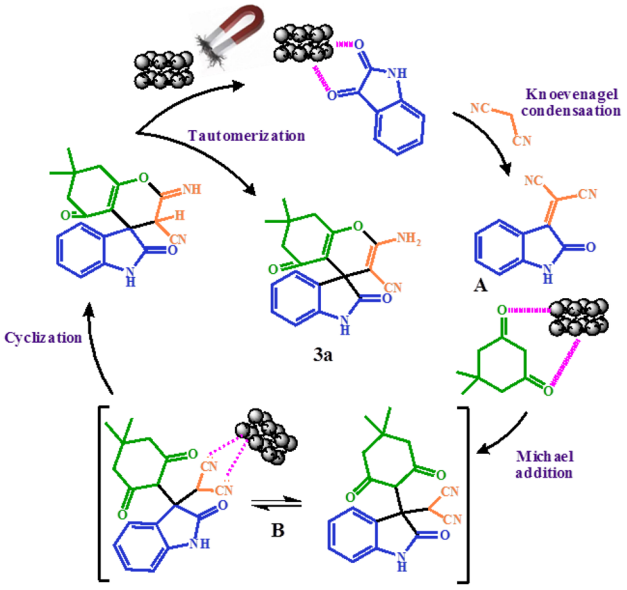

Fig. 12 The probable mechanism for the preparation of spirooxindole using $MnFe_2O_4$@SiO_2/APTPOSS

were subsequently washed with water and dried under vacuum at 60 °C for 24 h.

Preparation of octakis [3-(3 aminopropyltriethoxysilane) propyl] octasilsesquioxane (APTPOSS)

Under a nitrogen atmosphere, 2.07 g of ClPOSS (two mmol) and 4.43 g of 3-Aminopropyltriethoxysilane (20 mmol) were combined in a reaction vessel. The solution was stirred at 100 °C for two days, as illustrated in Fig. 3. Subsequently, the combination was allowed to cool to ambient temperature, followed by filtration of the solution and subsequent washing with methanol and acetone. The resulting product, APTPOSS, was obtained as a pale brown solid after drying under a vacuum and was stored for future use.

Preparation of $MnFe_2O_4$@SiO_2/APTPOSS MNPs

At first, 1.0 g of the magnetic manganese iron oxide that was produced was dispersed in a solution containing 1.6 ml of ammonium hydroxide, 10 ml of deionized water, and 30 ml of absolute ethanol using ultrasonic vibration for 20 min to create an active site for binding to $MnFe_2O_4$. Subsequently, 0.45 g of APTPOSS previously sonicated in deionized water, was added to this suspension. Following this, a mixture containing 0.9 ml of tetraethylorthosilicate diluted in ethanol (9 ml) was added dropwise to the suspension while continuously stirring at 80 °C. The reaction was allowed to progress for two days until it was completed, as shown in Fig. 3. The $MnFe_2O_4$@ SiO_2/APTPOSS product was then retrieved using a magnet after the mixture had cooled down. Afterward, the product was subjected to multiple washes with acetone and ethanol and dried in a vacuum at 70 °C.

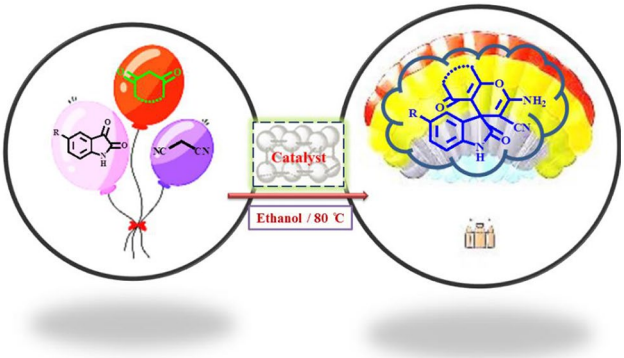

Fig. 13 An attractive outline of the reaction

A common procedure for the synthesis of (3a-n)

In a 50-ml round-bottom flask, one mmol each of Isatin derivatives, barbituric acid, dimedone or 4-hydroxy-coumarin, and malononitrile were mixed with 10 mg of the catalyst (MNPs@SiO_2/APTPOSS). The mixture was heated at 80 °C in the presence of ethanol until the reaction was complete. The progress of the reaction was monitored using thin-layer chromatography. The resulting products were purified by drying and washing with ethanol to obtain pure compounds (Fig. 13).

Abbreviations

MNPs	Magnetic nanoparticles.
APTPOSS	[3- (3-amino propyl triethoxysilane) propyl] octa-silsesquioxane.
TEM	Transmission electron microscopy.
SEM	Scanning Electron Microscopy.
VSM	Vibrating Sample Magnetometer.
FT-IR	Fourier transform infrared.
XRD	X-Ray diffraction.
CIPOSS	(3 chloropropyl) octasilsesquioxane.
TEOS	Tetraethyl Orthosilicate.
Ms	Saturation magnetization.
DMSO	Dimethyl sulfoxide.

Supplementary Information

The online version contains supplementary material available at https://doi.org/10.1186/s13065-024-01270-8.

Supplementary Material 1

Acknowledgements

The authors wish to thank the University of Kashan for providing facilities for this work.

Author contributions

Samira Moein Najafabadi: Investigation, Writing-Original draft preparation, Visualization.Javad Safaei Ghomi: Supervision, Conceptualization, Reviewing and Editing.

Funding

Not applicable.

Data availability

The data about this study is fully accessible in the published article and its supplementary information file.

Declarations

Ethics approval and consent to participate

Not applicable.

Consent for publication

Not Applicable.

Competing interests

The authors declare no competing interests.

Received: 23 April 2024 / Accepted: 15 August 2024
Published online: 24 August 2024

References

1. Sadeghzadeh SM, Zhiani R, Emrani S. Pd/APTPOSS@ KCC-1 as a new and efficient support catalyst for C–H activation. RSC adv. 2017;7:24885–94.
2. Miceli M, Frontera P, Macario A, Malara A. Recovery/reuse of heterogeneous supported spent catalysts. Catalysts. 2021;11:591.
3. Isfahani AL, Mohammadpoor-Baltork I, Mirkhani V, Khosropour AR, Moghadam M, Tangestaninejad S, Kia R. Palladium nanoparticles immobilized on nano-silica triazine dendritic polymer (Pdnp-nSTDP): an efficient and reusable catalyst for Suzuki–Miyaura cross-coupling and heck reactions. Adv Synth Catal. 2013;355:957–72.
4. Chadha U, Selvaraj SK, Ashokan H, Hariharan SP, Mathew Paul V, Venkatarangan V, Paramasivam V. Complex nanomaterials in catalysis for chemically significant applications: from synthesis and hydrocarbon processing to renewable energy applications. Adv Mater Sci Eng. 2022;2022:1–72.
5. Narayan N, Meiyazhagan A, Vajtai R. Metal nanoparticles as green catalysts. Mater. 2019;12:3602.
6. Dong Y, Xue F, Wei Y. Magnetic nanoparticles supported N-heterocyclic palladium complex: synthesis and catalytic evaluations in Suzuki cross-coupling reaction. J Phys Chem Solids. 2021;153:110007.
7. Vargas-Ortiz JR, Gonzalez C, Esquivel K. Magnetic iron nanoparticles: synthesis, surface enhancements, and biological challenges. Processes. 2022;10:2282.
8. Das SK, Chatterjee S, Bhunia S, Mondal A, Mitra P, Kumari V, Pradhan A, Bhaumik A. A new strongly paramagnetic cerium-containing microporous MOF for CO_2 fixation under ambient conditions. Dalton Trans. 2017;46:13783–92.
9. Basu S, Kayal U, Maity S, Ghosh P, Bhaumik A, Mukhopadhyay C. Utility of the Ditopic Nature of magnetically recyclable $NiFe_2O_4$ Nano-Catalyst for the Green synthesis of two different Spiro [indoline-pyrrolizine] scaffolds. ChemistrySelect. 2018;3:12755–63.
10. Mondal J, Sen T, Bhaumik A. Fe_3O_4@ mesoporous SBA-15: a robust and magnetically recoverable catalyst for one-pot synthesis of 3, 4-dihydropyrimidin-2 (1 H)-ones via the Biginelli reaction. Dalton Trans. 2012;41:6173–81.
11. Abu-Dief AM, Abdel-Fatah SM. Development and functionalization of magnetic nanoparticles as powerful and green catalysts for organic synthesis. Beni-Suef University. J Basic Appl Sci. 2018;7:55–67.

12. Rathnayake H, White J, Dawood S. Polysilsesquioxane-based organic-inorganic hybrid nanomaterials and their applications towards organic photovoltaics. Synth Met. 2021;273:116705.
13. Chen Y, Feng L, Sadeghzadeh SM. Reduction of 4-nitrophenol and 2-nitroaniline using immobilized $CoMn_2O_4$ NPs on lignin supported on FPS. RSC adv. 2020;10:19553–61.
14. Waki M, Mizoshita N, Tani T, Inagaki S. Periodic mesoporous organosilica derivatives bearing a high density of metal complexes on pore surfaces. Angew Chem. 2011;49:11871–5.
15. Kowalewska A. (2018) Self-assembly of POSS-containing materials. Polymer/POSS nanocomposites and hybrid materials: preparation, properties, applications, pp. 45–128.
16. Drobota M, Ursache S, Aflori M. Surface functionalities of polymers for biomaterial applications. Polym. 2022;14:2307.
17. Kim YB, Cho JW, Lee YJ, Bae D, Kim SK. High-index-contrast photonic structures: a versatile platform for photon manipulation. Light: Sci& Appl. 2022;11:316.
18. Sypabekova M, Hagemann A, Rho D, Kim S. 3-Aminopropyltriethoxysilane (APTES) deposition methods on oxide surfaces in solution and vapor phases for biosensing applications. Biosens. 2022;13:36.
19. Safaei-Ghomi J, Nazemzadeh SH, Shahbazi-Alavi H. Preparation and characterization of Fe_3O_4@ SiO_2/APTPOSS core–shell composite nanomagnetics as a novel family of reusable catalysts and their application in the one-pot synthesis of 1, 3-thiazolidin-4-one derivatives. Appl Organomet Chem. 2016;30:911–6.
20. Chadha N, Silakari O. Indoles as therapeutics of interest in medicinal chemistry: Bird's eye view. Eur J Med Chem. 2017;134:159–84.
21. Heravi MM, Amiri Z, Kafshdarzadeh K, Zadsirjan V. Synthesis of indole derivatives as prevalent moieties present in selected alkaloids. RSC adv. 2021;11:33540–612.
22. Sachdeva H, Mathur J, Guleria A. Indole derivatives as potential anticancer agents: a review. J Chil Chem Soc. 2020;65:4900–7.
23. Sravanthi TV, Manju SL. Indoles—A promising scaffold for drug development. Eur J Pharm Sci. 2016;91:1–0.
24. Gaikwad DD, Chapolikar AD, Devkate CG, Warad KD, Tayade AP, Pawar RP, Domb AJ. Synthesis of indazole motifs and their medicinal importance: an overview. Eur J Med Chem. 2015;90:707–31.
25. Ferrer L, Mindt M, Wendisch VF, Cankar K. (2023) Indoles and the advances in their biotechnological production for industrial applications. Syst Microbiol Biomanuf 1–17.
26. Almandil NB, Taha M, Gollapalli M, Rahim F, Ibrahim M, Mosaddik A, Anouar EH. Indole bearing thiadiazole analogs: synthesis, β-glucuronidase inhibition and molecular docking study. BMC Chem. 2019;13:1–0.
27. Moein Najafabadi S, Safaei Ghomi J. Synthesis of COF-SO_3H immobilized on manganese ferrite nanoparticles as an efficient nanocomposite in the preparation of spirooxindoles. Sci Rep. 2023;13:22731.
28. Heravi MM, Zadsirjan V. Prescribed drugs containing nitrogen heterocycles: an overview. RSC Adv. 2020;10:44247–311.
29. Oboudatian HS, Safaei-Ghomi J. Silica nanospheres KCC-1 as a good catalyst for the preparation of 2-amino-4H-chromenes by ultrasonic irradiation. Sci Rep. 2022;12:2381.
30. Nasri S, Bayat M, Farahani HV, Karami S. (2020) Synthesis of new functionalized thiazolo pyridine-fused and thiazolo pyridopyrimidine-fused spirooxindoles via one-pot reactions. Heliyon 6.
31. Panda SS, Girgis AS, Aziz MN, Bekheit MS. Spirooxindole: a versatile biologically active heterocyclic scaffold. Molecules. 2023;28:618.
32. Li MM, Duan CS, Yu YQ, Xu DZ. A general and efficient one-pot synthesis of spiro [2-amino-4H-pyrans] via tandem multi-component reactions catalyzed by Dabco-based ionic liquids. Dyes Pigm. 2018;150:202–6.
33. Zhiani R, Sadeghzadeh SM, Emrani S. Synthesis of spiroindenopyridazine-4 H-pyran derivatives using Cr-based catalyst complexes supported on KCC-1 in aqueous solution. RSC Adv. 2018;8:6259–66.
34. Ghasemzadeh MA, Mirhosseini-Eshkevari B, Abdollahi-Basir MH. Green synthesis of spiro [indoline-3, 4′-pyrano [2, 3-c] pyrazoles] using Fe_3O_4@ l-arginine as a robust and reusable catalyst. BMC Chem. 2019;13:119.
35. Ziarani GM, Moradi R, Lashgari N. Asymmetric synthesis of chiral oxindoles using isatin as starting material. Tetrahedron. 2018;74:1323–53.
36. Zhao H, Zhao Y. Engaging isatins and amino acids in multicomponent one-pot 1, 3-dipolar cycloaddition reactions—easy access to structural diversity. Molecules. 2023;28:6488.
37. Ren Y, Yang B, Liao X. The amino side chains do matter: chemoselectivity in the one-pot three-component synthesis of 2-amino-4 H-chromenes by supramolecular catalysis with amino-appended β-cyclodextrins (ACDs) in water. Catal Sci Technol. 2016;6:4283–93.
38. Toorbaf M, Moradi L. Preparation of GO/SiO_2/PEA as a new solid base catalyst for the green synthesis of some spirooxindole derivatives. RSC Adv. 2021;11:21840–50.
39. Abdolmohammadi S, Rasouli Nasrabadi SR, Dabiri MR, Banihashemi Jozdani SM. TiO_2 nanoparticles immobilized on Carbon nanotubes: an efficient heterogeneous Catalyst in Cyclocondensation reaction of Isatins with Malononitrile and 4-Hydroxycoumarin or 3, 4-Methylenedioxyphenol under mild reaction conditions. Appl Organomet Chem. 2020;34:5462.
40. Dittmar U, Hendan BJ, Flörke U, Marsmann HC. Funktionalisierte octa-(propylsilsesquioxane)(3-XC_3H_6) 8 (Si_8O_{12}) modellverbindungen für oberflächenmodifizierte kieselgele. J Organomet Chem. 1995;489:185–94.

Publisher's note